IEEE Access
Multidisciplinary | Rapid Review | Open Access Journal

SPECIAL SECTION ON ADVANCED MODELING AND CONTROL OF COMPLEX MECHATRONIC SYSTEMS WITH NONLINEARITY AND UNCERTAINTY

Received November 24, 2017, accepted January 7, 2018, date of publication January 18, 2018, date of current version February 28, 2018.

Digital Object Identifier 10.1109/ACCESS.2018.2795247

Stabilizing an Urban Semi-Autonomous Bicycle

M. RAMOS GARCÍA, DANIEL A. MÁNTARAS[1], JUAN C. ÁLVAREZ[2], AND DAVID BLANCO F.[3]

[1]Transportation Engineering and Infrastructure Area, Department of Construction and Manufacturing Engineering, University of Oviedo, 33204 Gijón, Spain
[2]Multisensor Systems and Robotics Laboratory (SiMuR), Department of Electrical and Computer Engineering, University of Oviedo, 33204 Gijón, Spain
[3]Engineering of Manufacturing Processes Area, Department of Construction and Manufacturing Engineering, University of Oviedo, 33204 Gijón, Spain

Corresponding author: M. Ramos García (232mario232@gmail.com)

ABSTRACT A comprehensive and a deep analysis on how to stabilize an urban semi-autonomous bicycle was carried out. Its more relevant aspects are presented in this paper. The resulting stabilized bicycle is intended to serve as a future evolution for the current bike-share programs. This bicycle would go to meet the user autonomously, and after that it could be used by the rider in the traditional fashion. Therefore, the resulting system must be stable throughout the entire operating speed range and must be rideable by a person when used in manual mode. A study of bicycle dynamics and stability control has led the way followed throughout this investigation. Consecutively, all the examined aspects are applied to introduce a few alternatives for solving the stability problem. One of them, the Alnilam concept, is further developed to unveil its possibilities. Furthermore, it has been successfully tested in a multibody co-simulation using Adams and Simulink, thus illustrating its behavior and testing its performance. The results of this simulation are very promising and encouraging to further develop this concept.

INDEX TERMS Bicycles, control design, stability, simulation, transportation.

I. INTRODUCTION

The stability of bicycles is an issue that has scarcely been understood in dynamics and is a commonly ignored problem. After two centuries of debate and unfinished modeling, new researches are paving the groundwork for increasing studies regarding this issue.

Throughout the last few decades, some researches have appeared thanks to new dynamics models and to the computational power available nowadays. Their purpose is to propose and test different alternatives to stabilize a bicycle. Despite their common goal of making a bicycle stable, they propose a wide variety of applications for their stabilized bicycles.

Although there have been numerous investigations regarding this aspect, the problem still seems to be unsolved. The designed systems are mostly only for autonomous purposes, making the bicycle unrideable by a person. Moreover, there is a lack of an integrated solution that allows the system to be stable throughout the entire operating speed range.

In this study, the stability problem is addressed to propose feasible approaches mainly from the hardware point of view. The approach taken must consider the speed range and its rideability.

The stabilized bicycle introduced in this paper is intended to be used as an urban semi-autonomous bicycle. Such system could be fully autonomous when going to pick up a rider and fully manual while being used by them.

This bicycle may be able to attend the demand of customers right in place, both when they start their commutes and when they end them.

The user of this system would just request a bicycle using their smartphone and the nearest one would come to meet them. After their commute, the user would leave the bicycle wherever they finish it, so that it would be available for the next nearest user. Such system makes a better match between offer and demand, thus improving current bike-share programs.

A deep study of bicycle dynamics and stability control is mandatory for proposing feasible solutions that meet all the requirements of the system.

II. BICYCLE DYNAMICS

Bicycles have been a difficult problem for dynamics since their invention back in 1817. Understanding the behavior and the stability of these systems is still an unsolved issue, but it is far nearer than a few decades ago.

The main action to stabilize a bicycle is still that which Rankine [1] mentioned in 1869 and some authors refer to it as the ''steer into the fall'' action. By turning into the fall, a centrifugal force is created that opposes the gravitational force due to the lean angle.

This action could be done by the rider but it could also be carried out by the bicycle itself as a complex and scarcely

understood result of its dynamics. This phenomenon is called self-stability.

In [2] and [3] there can be found comprehensive reviews of these topics and useful references to other important studies in this field.

A precise and robust dynamics model of the bicycle is needed for both the design and simulation phases. The chosen model was that described by Meijaard *et al.* [4] which is a very precise and experimentally validated model [5]. This so-called Whipple model – based on Whipple's work back in 1899 [6] – consists of four rigid bodies connected to each other by hinges, the four bodies being the rear frame, the rear wheel, the front wheel and the front frame.

The resulting model has 25 geometry and mass parameters and three degrees of freedom: forward speed v, lean rate $\dot{\emptyset}$ and steering rate $\dot{\delta}$. The final equations are linearized for small perturbations of the upright steady forward motion with $[\emptyset, \delta] = [0, 0]$.

The dynamics of the lateral and the forward motion are decoupled, the forward speed being constant. At a forward speed v, the linearized lateral dynamics equations are

$$M\ddot{q} + vC_1\dot{q} + \left[gK_0 + v^2K_2\right]q = f \qquad (1)$$

where the time-varying variables are $q = [\emptyset, \delta]^T$, the generalized torques $f = \left[T_\phi, T_\delta\right]^T$ and with M, C_1, K_0 and K_2 being constant matrices.

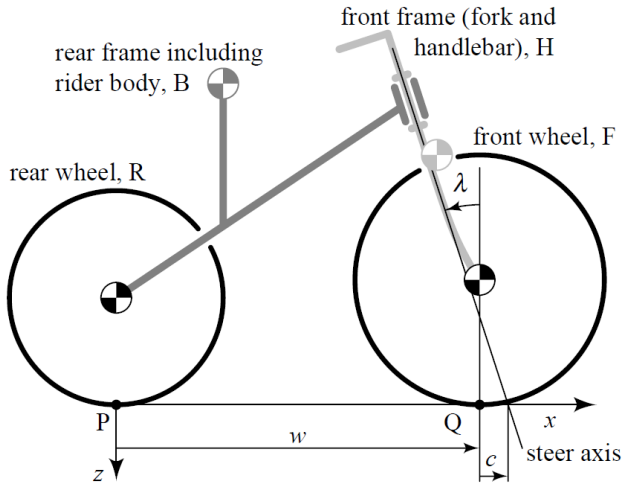

FIGURE 1. Whipple bicycle model parameters [4]. The four rigid bodies are represented by H, F, B and R. Other parameters are the wheelbase w, the steer axis tilt λ and the trail c.

A design application of this model was carried out by Kooijman *et al.* [7], checking the "Supporting online text material" is strongly recommended to understand more about the Whipple model and its characteristics.

With the linearized Whipple model, it is very useful to obtain the eigenvalues of the system with respect to the forward speed. In this way, the stability issues and the behavior of the system are observable through its eigenvalues and eigenmodes. As explained in [4], four eigenmodes are the most common and it is important to understand their behavior in order to solve the stability problem.

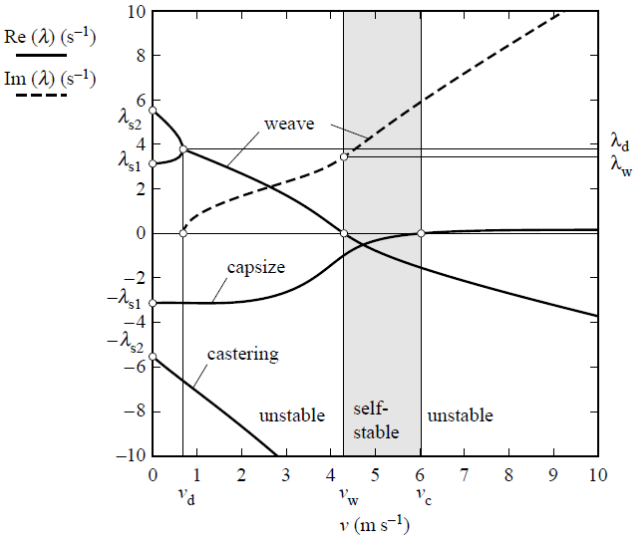

FIGURE 2. Eigenvalues with respect to the forward speed for the benchmark bicycle [4]. A self-stable behavior appears between the weave speed $v_W \approx 4.3$ m/s and the capsize speed $v_c \approx 6.0$ m/s. The four different eigenmodes of the system are also observable.

First, at near-zero speeds, there are two pairs of real eigenvalues corresponding to an inverted pendulum-like falling. Then, the castering mode is dominated by steer in which the front ground contact follows a tractrix-like pursuit trajectory. Finally, the most important are the weave mode and the capsize mode.

Steering sinuously about the headed direction with a phase lag relative to leaning is the characteristic behavior of the weave mode, while in the capsize mode it is dominated by the lean and, when unstable, makes the system lean progressively until it falls over.

Fig. 2 shows how from $v \approx 0.7$ m/s, the oscillatory weave motion emerges. Unstable first but stable between the weave speed and the capsize speed, this motion leads to a mildly unstable phase when the capsize eigenvalue crosses the origin.

In conclusion, the uncontrolled bicycle shows an asymptotically stable behavior between the weave and the capsize speed, in which all eigenvalues have negative real parts.

III. STABILITY CONTROL

Throughout the last couple of decades, there have been many attempts to make a stability control for bicycles. Different strategies have been used but no one seems to have come up with a full solution to the problem.

Only a few researches appear to be near to the solution. Unfortunately, the resulting system is neither a bicycle that could be used by a rider nor is it stable for the entire operating speed range.

Schwab and Meijaard [2] make a very comprehensive review of stability control and rider control, with useful

references both to rider actions and to stability control strategies.

Basically, there are three main strategies that have been used to control the stability of a bicycle.

A. STEERING

The first strategy is a steering control, with two different approaches: a steering torque control and a steering angle control. This control strategy seems to be the most natural and convenient, since it is the one that humans mainly use [8].

The principal limitation of this steering stability control is the forward speed of the system, as can be observed in [9] when the feedback gains go asymptotically to infinity when approaching a forward speed of $v = 1$ m/s.

This seems logical when thinking about the physical principle behind the stabilization effect of the ''steer into the fall'' action which is creating a centrifugal force. Therefore, the lower the speed, the less centrifugal force is created.

It can also be noticed when looking at the eigenvalues of the uncontrolled system with respect to the forward speed, as in the first range of speeds it shows an inverted pendulum-like falling behavior.

Nevertheless, with enough forward speed the steering control has shown very promising results both in simulations [9] and in experimental tests [10], and also in unstable and in self-stable speed ranges [11].

Despite the results, most of the tests on this steering stability control have been carried out at constant speeds or in very short speed ranges. Moreover, they are only valid for speeds higher than around 1 m/s, due to the above-mentioned reasons.

An illustrative and very advanced proof of the capabilities of such stability control was carried out recently at the Tsinghua University in China.

B. MOVING MASS

The second control strategy consists of using a moving mass.

It is commonly believed that the inverted pendulum-like movement of the rider's body is one of the main stabilization strategies used by human riders. However, almost all the research made in this regard agrees that this body movement plays quite an insignificant role in stabilizing the bicycle [8] and that riders hardly ever use it.

Therefore, this strategy is intended to stabilize the system with no speed or very little speed, as it is done to stabilize an inverted pendulum.

Two different approaches have been used in this stabilization strategy: a balancer and a flywheel.

Keo *et al.* [12] experimentally tested a bicycle-like system with a device that can be used both as a balancer and as a flywheel. The superior performance of the flywheel over the balancer is proven.

Apart from the appropriate speed range, the main problem with this kind of systems is that they are very invasive. This aspect normally makes them unusable for the rider.

C. ACTIVE GYRO

The last stabilization strategy consists in the use of an active gyro. As in the previous strategy, this is intended to control the stability at zero or near-zero speeds.

Just a few studies have tried this strategy [13], [14] and while giving decent experimental results, large and invasive assemblies were required.

D. SUMMARY

To sum up, there has been a lot of proposals tested to control the stability of a bicycle.

When there is enough forward speed, the problem seems to be solved with a steering control, but there are more reasonable doubts when it comes to lower speeds.

In order to solve this problem and obtain a fully stable bicycle, while maintaining its capability to be normally used by a rider, it seems to be necessary to implement a system that combines several strategies.

Such system must be able to stabilize the machine throughout the entire operating speed range while, at the same time, being as less invasive as possible to allow riders' normal use.

It is also important to pay attention to the role of the control algorithms that are used in each stability control strategy, as they can greatly improve the performance of a given hardware solution.

IV. SOLVING THE STABILITY PROBLEM

The main goal of this investigation is to propose feasible solutions to the stability problem of bicycles while maintaining their capability to be normally used by a rider.

Two possible solutions are introduced but not further developed after a preliminary study in which neither the proper performance nor the right implementation were found. The first is a bicycle with drone-like air propellers in the main frame creating lateral thrust to maintain the bicycle in the vertical position when the forward speed is low or zero.

The second consists of a bicycle with a wheeled retractile arm support system that maintains the vertical position of the bicycle while in zero or low speeds. In both cases, a steering control would take care of the stability at higher speeds.

A suspension-like system to allow some leaning while turning with the support system deployed and a lightweight, reliable and fast retraction/deployment mechanism are the main issues of this solution.

Nonetheless, this paper focuses on another solution for the stability problem, a combination of a retractile flywheel system and a steering control. In this case, a retractile flywheel will take care of the stability at zero or low speeds and as it is retractile it will allow the rider to use the system as usual. At higher speeds, the steering control will be in charge of the stability control with the flywheel steady but ready to be used.

This proposed system, from now on called Alnilam, presents a few challenges that will be addressed in the following sections.

A. THE CONCEPT OF ALNILAM

Here, the introduced concept will be further developed to test its possibilities and feasibility. The Alnilam bicycle will include a retractile flywheel to stabilize the system while it has the inverted pendulum-like behavior.

1) RETRACTILE FLYWHEEL

The flywheel will have a double-arm geometric configuration consisting of two rotating prismatic bodies that may be governed by either two actuators, or by one actuator and a coupling system.

When the flywheel is retracted into the bicycle's frame these two bodies must be firmly attached to the frame. When deployed, they have to be coupled with each other to create a flywheel-like motion.

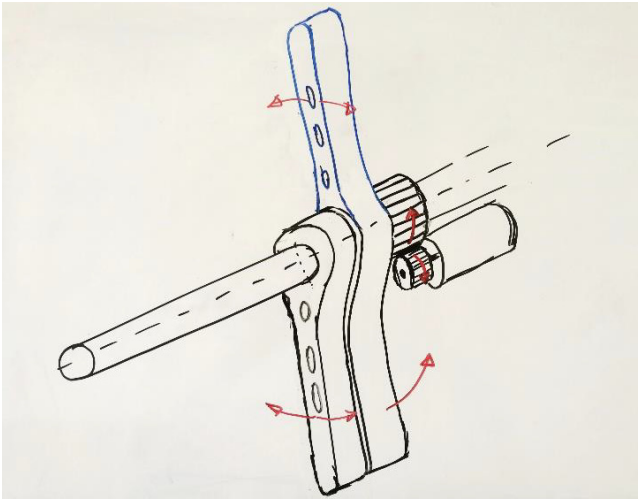

FIGURE 3. Sketch of the proposed conceptual design of the retractile flywheel system. In black is the retracted configuration with both bodies side to side. The deployed configuration appears in blue, the actuated body rotates 180° and couples to the other body. This coupled situation makes a flywheel-like system.

Considering that the one-actuator option is the best, many alternatives are available for making the coupling mechanism between the two bodies. A clutch would be a possibility but the one proposed here consists of a translating slender cylinder, actuated by a servomotor.

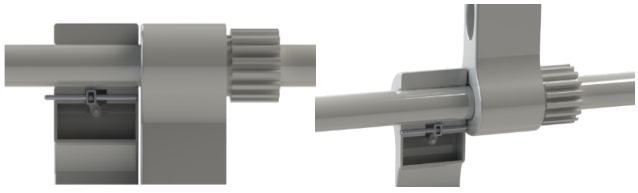

FIGURE 4. Simplified rendered image of the coupling system when the flywheel is retracted and when it is deployed.

This system would attach the non-actuated body to the frame when the flywheel is retracted and would couple both bodies when the flywheel is deployed. Another advantage of this possibility is that the coupling system would be embedded in one of the flywheel arms.

2) MASSES AND DIMENSIONS

To have a preliminary design of the proposed system, approximated dimensions and masses are necessary so that a simplified 3D model can be made for simulation purposes.

Overall dimensions of the Alnilam bicycle are chosen considering other urban bicycle designs, the ergonomics and the position of the rider.

Designing a bicycle with the proper reach-stack ratio and adequate component dimensions are aspects with a great impact both on ergonomics and maneuverability.

A list of bicycle maneuverability and stability referenced experiments can be found in Table 1 [2].

TABLE 1. Main overall dimensions.

Reach	375 mm
Stack [a]	460-600 mm
Head tube	100 mm
Steer axis tilt	72°
Trail	80 mm
Wheelbase	1000 mm
Standover height	790 mm
Wheel diameter	26" (660.4 mm)

[a]The stack dimension has two values depending on the way it is measured.

The simplified system consists of 5 bodies: the main assembly, the front assembly, the front and rear wheels, and the pedal assembly.

As can be seen, this is very similar to the structure of the Whipple model, but introducing the pedal assembly as an extra element because of its importance while studying the interference between components. A set of masses are supposed considering the characteristics of each assembly.

TABLE 2. Main overall masses.

Main assembly	10 kg
Front assembly	4 kg
Front wheel	4 kg
Rear wheel	2.2 kg
Pedal assembly	1.5 kg
Retractile flywheel [a]	?

[a]The retractile flywheel mass needs to be calculated to meet the stability requirements.

All masses are an assumption based on the elements that should be on each assembly. In the main assembly, there may be batteries, an actuator and the control electronics. Therefore, its mass will depend very much on the necessary autonomy of the system. In the front assembly, there should be some sensors and there may be an actuator for the steering control.

The difference between the mass of the front and the rear wheel comes from the electric motor being on the front wheel.

3) MODEL AND SIMULATION OF THE FLYWHEEL

In order to estimate the performance and the necessary characteristics of the flywheel system, a model of an inverted pendulum with a flywheel is used.

The model is derived using Lagrangian mechanics in a similar way to the derivations in [15] and [16].

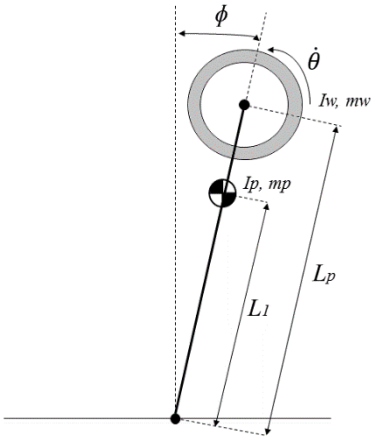

FIGURE 5. Inverted pendulum with flywheel diagram. ϕ is the lean angle, $\dot{\theta}$ is the rotational speed of the flywheel. I_p and M_p are the mass properties of the pendulum's CG and I_w and M_w are those of the flywheel. L_p and L_1 are the length of the pendulum and the distance between the center of rotation and the pendulum's CG.

Linearizing the model around the vertical position of the system, the two following coupled equations are obtained,

$$(\alpha_1 + I_w) \cdot \ddot{\phi} + I_w \cdot \ddot{\theta} = \alpha_2 \phi - C_1 \dot{\phi} \quad (2)$$

$$I_w \cdot \left(\ddot{\phi} + \ddot{\theta}\right) = T - C_2 \dot{\theta} \quad (3)$$

where,

$$\alpha_1 = m_P L_1^2 + Ip + m_w L_p^2$$
$$\alpha_2 = g \cdot \left(m_P L_1 + m_w L_p\right)$$

With T being the flywheel torque, and C_1 and C_2 being dissipative constants.

The model is now transformed into its state space form to design a controller and simulate various situations with different flywheel properties.

$$\dot{x} = Ax + Bu$$
$$x = \left[\phi, \dot{\phi}, \theta, \dot{\theta}\right]^T; \quad u = [T]$$
$$A = \begin{bmatrix} 0 & 1 & 0 & 0 \\ \frac{\alpha_2}{\alpha_1} & -\frac{c_1}{\alpha_1} & 0 & \frac{c_2}{\alpha_1} \\ 0 & 0 & 0 & 1 \\ -\frac{\alpha_2}{\alpha_1} & \frac{c_1}{\alpha_1} & 0 & -\frac{(\alpha_1 + I_w)}{\alpha_1 \cdot I_w} \cdot c_2 \end{bmatrix}; \; B = \begin{bmatrix} 0 \\ -\frac{1}{\alpha_1} \\ 0 \\ \frac{\alpha_1 + I_w}{\alpha_1 \cdot I_w} \end{bmatrix} \quad (4)$$

For simulation purposes, a model of an inverted pendulum with a prismatic-type flywheel is created in Simscape/Simmechanics® (Simulink®).

A full-state feedback LQR is designed to control the flywheel's torque of the multi-body plant. With the mass of the entire system but the flywheel as a property of the pendulum and the height of the CG as if it were the bicycle, a few masses are tested for the flywheel.

The LQR is chosen and maintained after a few tests so that the only difference between simulations is the actual mass of the flywheel. The Q and R matrices are:

$$Q = \begin{bmatrix} 100 & 0 & 0 & 0 \\ 0 & 10 & 0 & 0 \\ 0 & 0 & 1 & 0 \\ 0 & 0 & 0 & 1 \end{bmatrix}; \quad R = [0.1] \quad (5)$$

The length of the flywheel arms is chosen not to be higher than handlebar's length, preventing the system from hitting external bodies.

In addition, the moment of inertia of the flywheel arms is calculated to be conservative. This allows improving this aspect without adding weight to the flywheel by positioning the CGs of the arms farther from their center of rotation.

Two types of simulations were carried out with a range of flywheel weights from 5 to 10 kg. One is a step impulse in the lean angle whereas the other is a white-noise perturbation also in the lean angle.

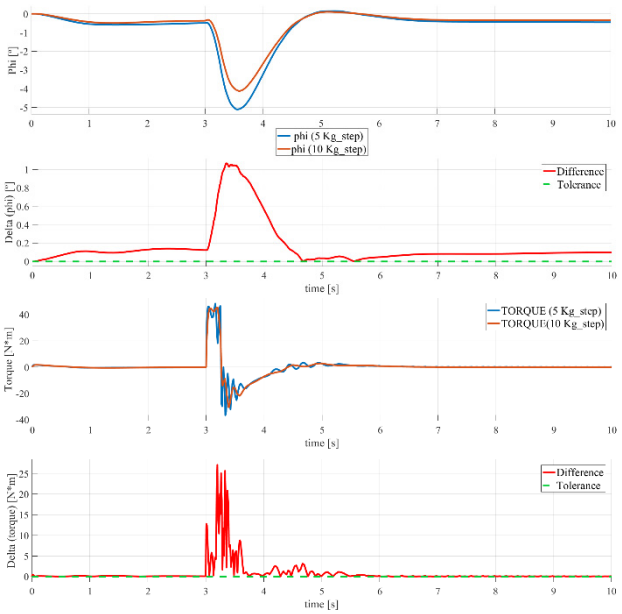

FIGURE 6. Simulation results of the inverted pendulum stabilization with a prismatic flywheel. The first two are the inclination angle response to a step perturbation and the comparison between a flywheel with 5 and 10 kg of mass. The following two are the torque introduce in the flywheel by the LQR control and its comparison between the two flywheel masses.

As was expected, both flywheel masses are able to stabilize the system. However, there is a difference of 1° in the maximum inclination value between them.

Regarding the torque, it can be observed that in the case of a 10 kg flywheel, its signal has less noise, is more constant and cleaner.

In the white-noise perturbation simulation, the results point to a similar conclusion. They show a little more inclination when the mass of the flywheel is smaller and a little more noise in the input torque.

For the concept design, a flywheel mass of 7.5 kg is chosen, as it is in a mid-range between the simulated ones and quite

feasible for the proposed concept bicycle. This flywheel mass makes an equivalent moment of inertia of 0.1501 kg · m^2, which could be reached with less mass.

4) OVERALL DESIGN

In regard to the position of this double-arm flywheel, it is important to consider a few aspects.

Its center has to be near the vertical of the system's CG to make the flywheel more efficient in stabilizing the bicycle as it would be in the ideal case of a simplified inverted pendulum model.

Moreover, a separation has to be kept to the handlebar to allow the necessary range of steering angle without colliding with the flywheel.

In addition, more considerations need to be taken such as leaving space for the flywheel motor and avoiding interferences with the seat and the down-tube.

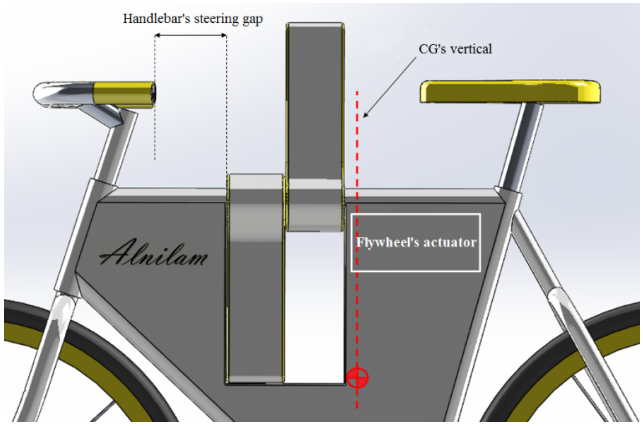

FIGURE 7. Rendered image of the flywheel position in Alnilam's 3D concept model.

A 3D model of Alnilam is made with all these properties and a few aesthetic aspects. The purpose of this 3D model is to obtain the inertial properties of the bicycle to introduce them into the linearized Whipple model and calculate the hypothetical behavior of the system.

Furthermore, the geometrical and inertial information of this 3D model will be used to simulate the system in a multibody dynamics software.

As can be noticed, the main frame is covered allowing it to have the batteries and the necessary hardware protected as well as the retracted flywheel integrated.

The design of the flywheel arms is a concept of a geometry that optimizes the moment of inertia with respect to the weight.

An important issue that should be considered in more advanced development phases is the proper lateral shape of these flywheel arms regarding their aerodynamics. As these bodies are going to rotate like a fan, it would be convenient to study the aerodynamic perturbations created by their rotation and try to minimize the rotating drag these arms will create.

For the Whipple model of Alnilam, the JBike6 is used. This software is available online thanks to Schwab *et al.* [17].

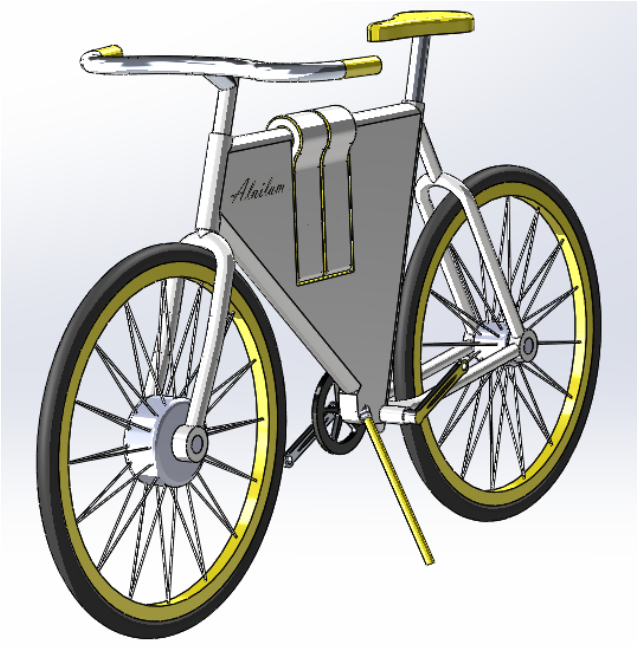

FIGURE 8. Alnilam's concept 3D model picture. Here the flywheel is retracted and the bicycle is supported by the kickstand.

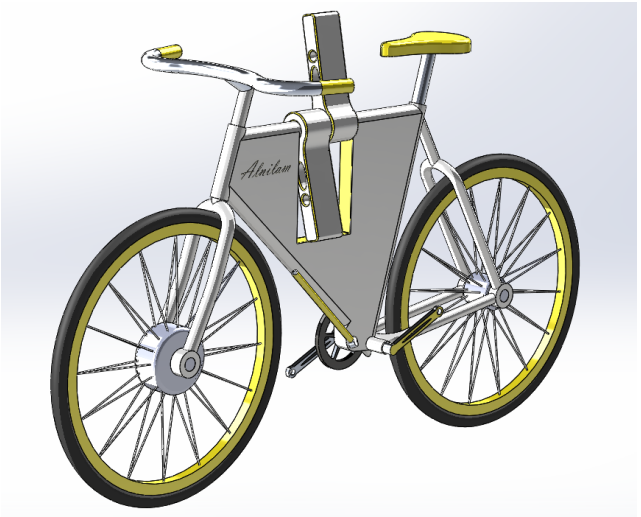

FIGURE 9. Alnilam's concept 3D model picture. Here the flywheel is deployed so the kickstand is retracted.

Filling the geometric and mass properties of Alnilam in the software, the open-loop eigenvalues versus the forward speed plot is obtained.

Although the system is never self-stable it is mildly stable for speeds higher than 4.5 m/s. Making some little adjustments in the positions of the CG of the different assemblies is quite easy to give it a self-stable zone.

Nevertheless, the priority in this respect would be to decrease the weave speed due to safety and handling related issues.

Despite the fact that the relationship between the handling and maneuverability, and the self-stability has never been

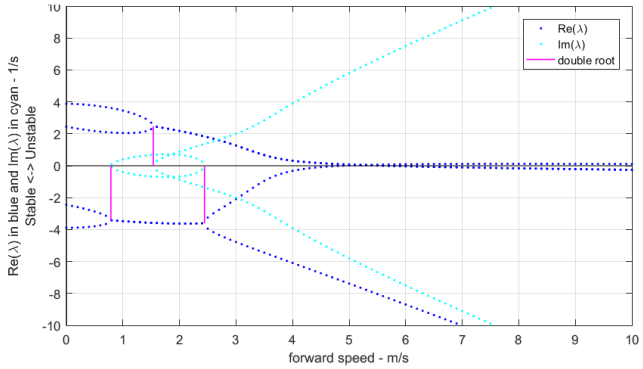

FIGURE 10. Eigenvalues of the open-loop linearized Whipple model for the Alnilam concept with respect to the forward speed. As can be seen, there is no weave or capsize speed as the system is never self-stable.

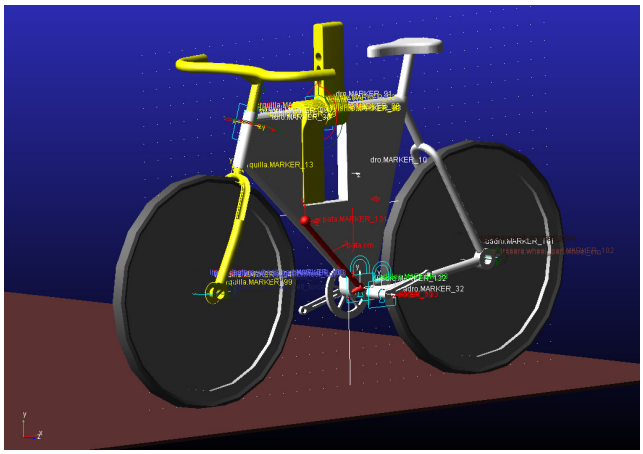

FIGURE 11. Picture of the concept model of Alnilam in Adams/View®. Notice that the wheels are different with respect to the 3D model because of the implementation of the Adams/Car® tires.

TABLE 3. I/O for the Adams® controls plant.

Inputs	Outputs
Front wheel torque	Forward speed
Steering torque	Lean angle
Flywheel torque	Lean rate
	Steering angle
	Steering rate
	Flywheel angle
	Flywheel speed

proved [2], the more stable the system is, the less stability control effort the rider has to undertake.

The operational speed in urban cycling commutes is between 16 and 18 km/h [18], which is a speed of around 5 m/s. Taking into account the average operational speed and the risks of an autonomous-driven bicycle, the top operational speed of the range of such system would not be much higher than 5 m/s.

In addition, it must be considered that the autonomous part of the operation should be short if there are enough bicycles throughout the city.

V. SIMULATION

Simulations were carried out in order to test and illustrate the possibilities of the Alnilam concept. For these simulations, Adams®, a multi-body dynamics software, was used in co-simulation with Simulink®, a control software.

The plant was created in Adams/View® exporting the geometries from the 3D model and configuring the inertial properties. A pair of modified Adams/Car® motorcycle tires were added to allow the proper movement of the bicycle.

The modifications were made focusing on its geometric properties and its dynamic behavior by modifying its Pacejka coefficients [19] to adapt them to the weight of the bicycle.

With all the proper joints and markers, the plant is exported as a controls plant specifying its inputs and outputs, to be controlled by a Matlab/Simulink® program.

A. CONTROL

A control program was developed in Matlab/Simulink® using the above-mentioned model as the controlled plant.

The control system has two feedback threads, one for the flywheel control and the other for the steering control.

First, the flywheel control has two different algorithms depending on whether it is controlling the stability of the system or just its position.

If the system is in the speed range in which the flywheel is in charge of the stability, a full-state feedback LQR control is active. This LQR is based on that designed with the inverted pendulum plus flywheel model described in the previous chapter.

On the contrary, if the system is in the speed range in which the stability is controlled by the steering, a full-state feedback LQR was designed to put the flywheel in its neutral position and maintain it there. This is also done at a low speed and with a low torque to minimize disturbances in the stability of the system.

Regarding the steering control, it also has two different control algorithms.

On the one hand, when the system's stability is controlled by the flywheel, the steering control is just a position control. This allows turning the bicycle in the simulation when the flywheel stability control is activated, thus testing its capabilities.

On the other hand, when the bicycle's stability is controlled by the steering torque, an intuitive control is active. This intuitive control was proposed by Schwab *et al.* in [9] and it is based on the "steer into the fall" principle governed by the expressions, $T_\delta = -K_v(v_{max} - v)\dot{\phi}$ for $v < v_{max}$, and $T_\delta = -K_c(v - v_{max})\phi$ for $v \geq v_{max}$. v_{max} is the switching speed between the two control law expressions, usually in the stable speed range, and K_v and K_c are constants defining the feedback gains.

In order to adjust this intuitive control, fig. 10 was used to see the theoretical behavior of the system in its different speed ranges.

With the information of the eigenvalues and after running some tests, it was decided that $v_{max} = 6$ m/s,

$K_v = -8$ N · s^2/rad and $K_c = -0.2$ N · s/rad. It was also decided that the speed at which the stability control changes between the flywheel control and the steering control will be $v_t = 2.25$ m/s.

Note that the v_{max} should never be reached as was discussed at the end of Chapter IV.

B. CO-SIMULATION SETUP

A few simulations were performed to test the system and adjust its control parameters and algorithms.

After that, a complete simulation was carried out to test various concatenated scenarios. These scenarios (fig. 12) are challenging to the system while likely to happen in its operational routine.

In the stationary plus steering perturbations scenario, the stability of the system is perturbed by a steering action to both sides with zero speed.

Regarding the concatenated inclination perturbations situation, the bicycle inclination is perturbed through the lean rate signal that the intuitive control uses as feedback when it is below the v_{max}.

The tight 180° turn is a situation in which the system has to face a large steering input at a low speed, testing the performance of the flywheel with a large lean angle.

Both high acceleration and deceleration situations are not likely to happen unless in an emergency case. The same goes for the high-speed situation, as has been discussed in a previous chapter.

At the end of the simulation, the system has to stabilize itself with the flywheel.

This situation tests how the flywheel is able to address the change of control system and how it corrects the possible inherited lean angle from the intuitive control.

By combining three open-loop inputs, the co-simulation is set up to make these scenarios. These three are the front wheel torque input, a steering angle input and a steering rate input.

The first is just an open-loop signal that goes directly to the torque input of the controls plant. The second goes to the steering angle control when the flywheel is in charge of the stability. The last one goes to the steering stability control when it is under v_{max} as a perturbation of the feedback signal which is the lean rate.

C. RESULTS AND DISCUSSION

The results will be analyzed using the numbers from fig. 12 to identify the different scenarios.

Due to the marker's rotation in the Adams® simulation, the inclination angle output from the Controls Plant places its new zero – the vertical position – in 180° from the point where the system turns and the global speed direction opposes the previous one.

This issue is solved with the control algorithm in order to allow the system to properly actuate after the 180° turn. Nonetheless, the signal shows an alteration exactly in the middle of the turn that instantaneously affects the proper co-simulation behavior. This alteration is highlighted with a red dashed box in the figures.

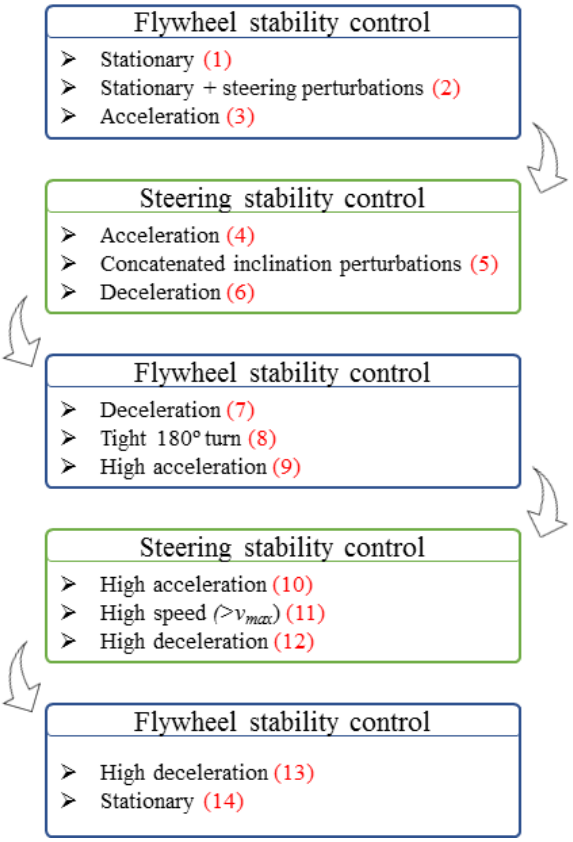

FIGURE 12. Simulation scenarios listed as they happen in the simulation. Numbers in red are for better interpretation of the results.

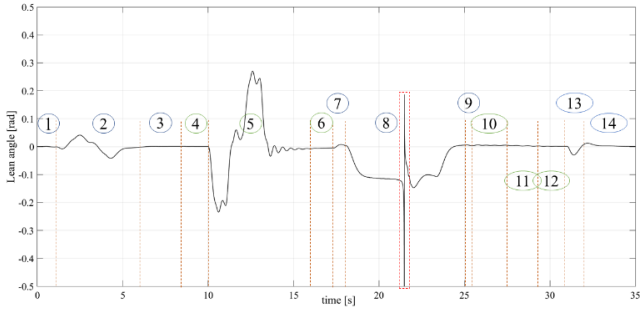

FIGURE 13. Lean angle in radians versus time in seconds of the Alnilam concept in the co-simulation.

The main aspect to pay attention to is the inclination of the bicycle.

Fig. 13 shows how this aspect behaves through the simulation. As can be observed, the system remains stable throughout the entire simulation.

The maximum lean angle is reached in the fifth scenario with a peak value of 14° because of the large lean rate input that was imposed, severely testing the ability of the intuitive control.

In the second scenario, the flywheel stability control is able to maintain the inclination angle between ±2°.

For the 8th scenario, the flywheel manages to keep a top inclination angle of 8° while making the 180° turn.

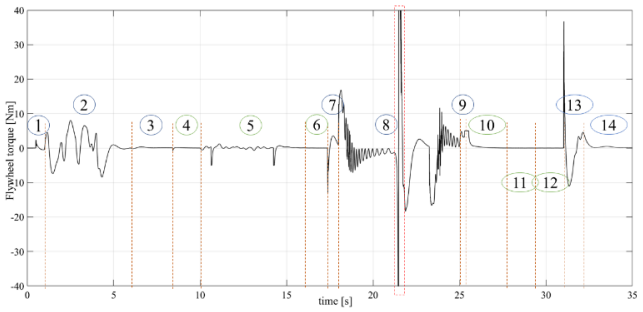

FIGURE 14. Flywheel torque in N · m versus time in seconds of the Alnilam concept in the co-simulation.

Another parameter worth consideration is the flywheel torque. Fig. 14 shows how this controlled input behaves throughout the simulation.

The demanded torque values are quite moderated. In the second scenario, the control does not demand more than 9 N · m while in the case of the 180° turn it has an 18 N · m peak value.

At the beginning of the 13th scenario, a high peak of torque is demanded caused by the sudden state values input in the LQR control.

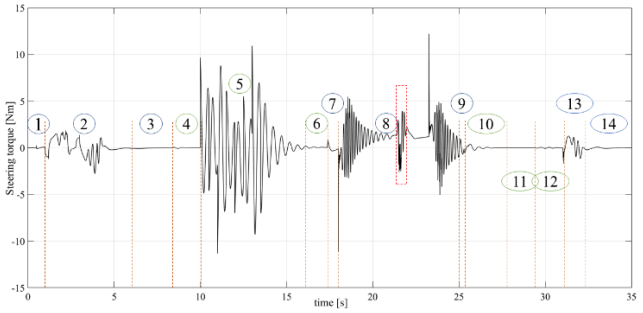

FIGURE 15. Steering torque in N · m versus time in seconds of the Alnilam concept in the co-simulation.

In regard to the steering torque input, shown in fig. 15, it is important to differentiate between the intuitive control parts and the steering angle control parts. The steering angle control was not properly designed to meet reasonable performance standards.

Looking at the steering stability control scenarios it can be noticed that the torque values required to stabilize the system are very low.

The only exception to that is the fifth scenario, in which the steering torque demanded is far higher due to the extreme situation created. It can be seen how the intuitive control noticeably oscillates while trying to reach the high lean rate imposed.

Other important aspects of the simulation are the steering angle, the rotational speed of the flywheel and the forward speed of the bicycle.

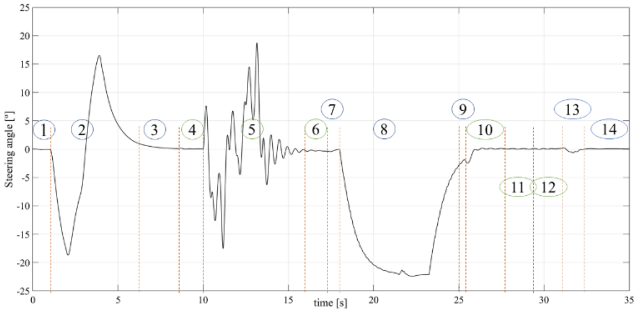

FIGURE 16. Steering angle in degrees versus time in seconds of the Alnilam concept in the co-simulation.

As can be seen in fig. 16, the steering angles of the system are quite large, thus creating unlikely adverse scenarios for the system's real-life situations.

It is interesting to notice how the intuitive control makes a counter-steer maneuver to create the necessary inclination angle in the fifth scenario.

Probably the most arguable aspect of this simulation is the rotational speed of the flywheel shown in fig. 17. The speeds of the flywheel are quite high for a normal and safe operation.

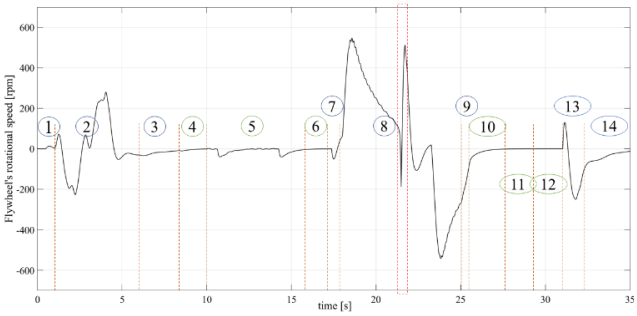

FIGURE 17. The rotational speed of the flywheel in rpm versus time in seconds of the Alnilam concept in the co-simulation.

This aspect should be further studied in order to get more reasonable speed values in the flywheel. A better-designed control with this issue in mind could be the first step towards a solution.

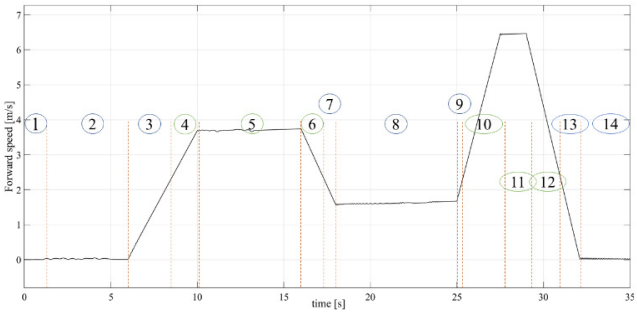

FIGURE 18. Forward speed in m/s versus time in seconds of the Alnilam concept in the co-simulation.

Regarding the forward speed shown in fig. 18, it can be noticed how the system faces the entire operating speed range.

Moreover, it is tested at even higher forward speed values in scenarios 10, 11 and 12.

An animation was also generated by the co-simulation. This animation is available along with this article, within an explanatory video. It is worth checking it out to see the performance of the system in a different and more visual way.

To sum up, the co-simulation shows the capabilities of the proposed system facing different situations. The results are very good and promising to further develop this Alnilam concept.

VI. CONCLUSIONS

A study of the bicycle stability problem was carried out to propose feasible solutions to stabilize it. This stabilized bicycle could be used as an urban semi-autonomous bicycle.

Such system may be able to be either fully autonomous or fully manual, like a standard urban bicycle.

The use of urban semi-autonomous bicycles might be an evolution for current bike-share programs and may result in an improvement in urban transportation.

A comprehensive study of the bicycle dynamics and control topics was mandatory. The conclusions drawn from this analysis are the stepping stones to the proposed solutions of the stability problem.

The proposed Alnilam concept was further developed to unveil its possibilities. At the same time, the other introduced proposals may help new ideas to be born.

Moreover, Alnilam was successfully stabilized in a multibody co-simulation. The stability is controlled by two different systems working at different speed ranges.

The proposed bicycle is capable of being used by a rider in a normal way. Furthermore, this stabilization was achieved throughout the entire operating speed range and while facing various challenging scenarios.

These promising results are a good step towards a further development of this idea.

It is hoped that all the work presented in this paper will prove deeply helpful in the future development of a system of this kind.

REFERENCES

[1] W. J. Rankine, "On the dynamical principles of the motion of velocipedes," *Eng.*, vol. 28, pp. 79, 129, 153, and 175, 1869.

[2] A. L. Schwab and J. P. Meijaard, "A review on bicycle dynamics and rider control," *Veh. Syst. Dyn.*, vol. 51, no. 7, pp. 1059–1090, 2013.

[3] J. P. Meijaard, J. M. Papadopoulos, A. Ruina, and A. L. Schwab, "Historical review of thoughts on bicycle self-stability," *Sci. Mag.*, Apr. 2011.

[4] J. P. Meijaard, J. M. Papadopoulos, A. Ruina, and A. L. Schwab, "Linearized dynamics equations for the balance and steer of a bicycle: A benchmark and review," *Proc. Roy. Soc. A, Math., Phys. Eng. Sci.*, vol. 463, no. 2084, pp. 1955–1982, 2007.

[5] J. D. G. Kooijman, A. L. Schwab, and J. P. Meijaard, "Experimental validation of a model of an uncontrolled bicycle," *Multibody Syst. Dyn.*, vol. 19, nos. 1–2, pp. 115–132, 2008.

[6] F. J. W. Whipple, "The stability of the motion of a bicycle," *Quart. J. Pure Appl. Math.*, vol. 30, pp. 312–348, Mar. 2017.

[7] J. D. Kooijman, J. P. Meijaard, J. M. Papadopoulos, A. Ruina, and A. L. Schwab, "A bicycle can be self-stable without gyroscopic or caster effects," *Science*, vol. 332, no. 5, pp. 339–342, 2011.

[8] J. D. G. Kooijman, A. L. Schwab, and J. K. Moore, "Some observations on human control of a bicycle," in *Proc. ASME Int. Design Eng. Tech. Conf. Comput. Inf. Eng. Conf. (IDETC/CIE)*, 2009, pp. 1–8.

[9] A. L. Schwab, J. D. G. Kooijman, and J. P. Meijaard, "Some recent developments in bicycle dynamics and control," in *Proc. 4th Eur. Conf. Struct. Control (4ECSC)*, 2008, pp. 695–702.

[10] V. Cerone, D. Andreo, M. Larsson, and D. Regruto, "Stabilization of a riderless bicycle [applications of control]," *IEEE Control Syst.*, vol. 30, no. 5, pp. 23–32, Oct. 2010.

[11] B. Michini and S. Torrez, "Autonomous stability control of a moving bicycle," in *Proc. Amer. Inst. Aeronaut. Astronaut.*, 2006, pp. 1–10.

[12] L. Keo, K. Yoshino, M. Kawaguchi, and M. Yamakita, "Experimental results for stabilizing of a bicycle with a flywheel balancer," in *Proc. IEEE Int. Conf. Robot. Autom.*, May 2011, pp. 6150–6155.

[13] B. T. Thanh and M. Parnichkun, "Balancing control of bicyrobo by particle swarm optimization-based structure-specified mixed H2/∞ control," *Int. J. Adv. Robot. Syst.*, vol. 5, no. 4, pp. 395–402, 2008.

[14] H. Yetkin, S. Kalouche, M. Vernier, G. Colvin, K. Redmill, and U. Ozguner, "Gyroscopic stabilization of an unmanned bicycle," in *Proc. Amer. Control Conf.*, Jun. 2015, pp. 4549–4554.

[15] X.-G. Ruan and Y.-F. Wang, "The modelling and control of flywheel inverted pendulum system," in *Proc. 3rd IEEE Int. Conf. Comput. Sci. Inf. Technol.*, Jul. 2010, pp. 423–427.

[16] M. Olivares and P. Albertos, "On the linear control of underactuated systems: The flywheel inverted pendulum," in *Proc. IEEE Int. Conf. Control Autom. (ICCA)*, Jun. 2013, pp. 27–32.

[17] A. L. Schwab, J. M. Papadopoulos, A. Ruina, and Dressel. JBike6. Delft University of Technology Cornell University. Accessed: Mar. 14, 2017. [Online]. Available: http://ruina.tam.cornell.edu/research/topics/bicycle_mechanics/JBike6_web_folder/index.htm

[18] P. Schepers, D. Twisk, E. Fishman, A. Fyhri, and A. Jensen, "The Dutch road to a high level of cycling safety," *Safety Sci.*, vol. 92, pp. 264–273, Feb. 2017.

[19] H. Pacejka, *Tire and Vehicle Dynamics*, 3rd ed. London, U.K.: Butterworth, 2012.

M. RAMOS GARCÍA was born in Avilés, Spain, in 1992. He received the B.S. degree in mechanical engineering and the M.S. degree in mechatronics engineering from the University of Oviedo, Spain, in 2015 and 2017, respectively.

He has experience in mechanical design, vehicle design and dynamics, 3-D printing, and mechatronics. His interests are related with his experience and with a strong focus on innovation and disruptive technologies. He has an inquisitive mind with interests in other fields such as space, physics, economics, technology, psychology, and political philosophy.

DANIEL A. MÁNTARAS was born in Gijón, Spain, in 1972. He received the M.S. degree in mechanical engineering from the University of Oviedo, Spain, in 1997, the M.S. degree in vehicle engineering from the Polytechnic University of Madrid, Spain, in 2000, and the Ph.D. degree in mechanical engineering from the University of Oviedo in 2001.

He has been a Professor of vehicle and transportation engineering with the University of Oviedo, since 2003. He has authored five books and over 50 scientific publications in conference proceedings and international peer-reviewed journals. His research interests include computer simulation, vehicle dynamics, accident reconstruction, and automotive safety.

JUAN C. ÁLVAREZ received the M.S. and Ph.D. degrees from the University of Oviedo in 1992 and 1998, respectively, after spending a year under the supervision of V. Lumelsky.

He has been a Teacher of control systems and robotics with the Department of Electrical, Electronics, Computers and Systems Engineering, University of Oviedo (UO), Gijón, since 2000, where he has been coordinating the Multisensor Systems and Robotics Laboratory (SiMUR) since 2001 and has been a Counselor of the IEEE Student Branch since 2008. He was a Co-Founder of the European Erasmus Mundus Master of Mechatronics and Micro-Mechatronic Systems (EU4M) and was the first Director of EU4M, UO, from 2004 to 2009. He is currently an Associate Professor of systems engineering and automation with UO. He served as the Vice President for the IEEE Robotics and Automation Spanish Branch and in the direction team of the department from 2008 to 2012.

He has authored over 40 papers in international journals, books, and refereed conferences. His research interests revolve around understanding motion: sensor-based robot motion planning and ambulatory human motion monitoring. He is on the editorial board of several scientific journals in those topics. His current research focus is on the development of wearable sensor systems able to interpret human motion as actions and intentions, in order to capture the interactions taking place in human–robots shared environments.

DAVID BLANCO F. was born in Oviedo, Asturias, Spain, in 1973. He received the M.S degree in indutrial engineering (Level 7–EQF) and Ph.D. degree in design and manufacturing from the University of Oviedo (UO), Spain.

He is currently an Associate Professor with the Department of Manufacturing Engineering, UO. He is currently leading the advanced research with the Additive Manufacturing Group, Gijón, Spain, and coordinating the master's in mechatronic engineering with the International Graduate Center, UO. He focused on over 40 research and development projects, encompassing public and private funding. He has authored 28 research articles. His current research interests include optimization of additive manufacturing processes, metrology and quality assessment of manufactured parts, and development of spectroscopic techniques and equipment for impurity control in fluids.